Iranian Journal of Materials Science and Engineering, Vol. 21, Number 3, September 2024
RESEARCH PAPER

Effect of Potassium Hydroxide Concentration and Activation Time on Rice Husk-Activated Carbon for Water Vapor Adsorption

Dewi Qurrota A'yuni[1], Hadiantono Hadiantono[1], Velny Velny[1], Agus Subagio[2], Moh. Djaeni[1,*], Nandang Mufti[3]

* *moh.djaeni@live.undip.ac.id*

[1] Department of Chemical Engineering, Faculty of Engineering, Universitas Diponegoro
[2] Department of Physics, Faculty of Science and Mathematics, Universitas Diponegoro Jl. Prof. Soedarto Tembalang, Semarang, Central Java, Indonesia 50275
[3] Department of Physics, Faculty of Mathematics and Science, Universitas Negeri Malang Jl. Semarang No.5, Sumbersari, Lowokwaru, Malang, East Java 65145

Received: February 2024 Revised: June 2024 Accepted: August 2024
DOI: 10.22068/ijmse.3522

Abstract: *Rice husk carbon by-products from industrial combustion are a promising source to produce a vast amount of activated carbon adsorbent. This research prepared rice husk-activated carbon adsorbent by varying the concentration of potassium hydroxide solution (5, 10, 15, 20% w/v) and activation time (2, 4, 6, 8 hours). Fourier-transform infrared (FTIR) spectral characterization indicated a significant effect before and after activation, especially the presence of hydroxyl groups. Based on the iodine adsorption, the specific surface area of the produced-activated carbon was approximately 615 m^2/g. Experimental results showed that increasing potassium hydroxide concentration and activation time increases the water vapor adsorption capacity of the activated carbon. Compared with the rice husk carbon, the KOH-activated carbon enhanced the water vapor adsorption capacity to 931%. In the adsorption observation, changing the temperature from 15 to 27°C caused a higher water vapor uptake onto the activated carbon. Two adsorption kinetics (pseudo-first- and pseudo-second-order models) were used to evaluate the adsorption mechanism. This research found that rice husk-activated carbon performed a higher water vapor adsorption capacity than other adsorbents (silica gel, zeolite, and commercially activated carbon).*

Keywords: *Activated carbon, Adsorption kinetics, Desiccant, Rice husk, Water vapor adsorption.*

1. INTRODUCTION

Water vapor adsorption is an essential process in several industrial practices, such as water harvesting [1], dehumidification [2], and desalination. As an example, in the dehumidification drying process, reducing water vapor from air enhances the driving force, which can shorten the drying time and retain heat-sensitive ingredients in the food product [3]. This is due to the significant difference between the concentration of water vapor on the food's surface and the air as the drying medium. Then, the mass transfer of water vapor from the product to the air can be fastened.

The need for water vapor adsorption led to the production of efficient materials for moisture control. Some studies presented different types of water adsorbents, including Covalent Organic Frameworks [4], Metal-Organic Frameworks (MOFs) [5], zeolite [6], silica gel [7], mesoporous silica [8], and activated carbon [9]. Covalent Organic Frameworks (COFs) and Metal-Organic Frameworks (MOFs) are mostly used in the water harvesting process because of their remarkable adsorption properties, which are highly tunable and high porosity [10]. However, those materials require careful handling due to potential structural damage and complex synthesis processes, making them relatively higher cost compared to other adsorbents [11]. Meanwhile, widely known water vapor adsorbents or desiccants (zeolite, silica gel, and activated carbon) are easily regenerated and more stable in structure.

There are several requirements in the adsorbent selection, including toxicity, adsorption capacity, cycles, and easiness in regeneration using low heat energy. Activated carbon is a non-toxic and thermally stable adsorbent with a high water adsorption capacity due to its large surface area [12]. Also, activated carbon can be produced from natural sources such as agricultural by-products. Thus, activated carbon is a promising adsorbent due to its abundance, low cost, and potential for sustainable water vapor removal.

Rice husk is a natural adsorbent that has been applied for various applications, including heavy metal and dye removal in wastewater [13, 14],

[DOI: 10.22068/ijmse.3522]

CO_2 adsorption [2], and urine purification [15]. In its application as a water vapor adsorbent, rice husk was exploited by Warsiki et al. [16] that produce rice husk-$CaCl_2$ composite desiccant. They reported that environmental humidity (water activity) and temperature influenced the adsorption capacity of the adsorbent. However, the study did not compare rice husk-$CaCl_2$ adsorption with other adsorbents. Moreover, untreated rice husk still contains contaminants in its pores and thus is still low in adsorption capacity. Another research showed that rice husk silica had the potential as a silica gel substitute in water vapor adsorption [17]. The adsorption mechanism of rice husk silica and silica gel was similar and affected by silanol groups on their surface. Nevertheless, commercial silica adsorbed twice as much water vapor than silica produced from rice husk. Therefore, this research focuses on synthesizing natural-based adsorbent with high water vapor adsorption.

This work aims to produce activated carbon from rice husk as a water vapor adsorbent and its comparison with other commercial adsorbents (commercial activated carbon, silica gel, and zeolite). In the process, several studies used potassium hydroxide, zinc chloride, hydrochloric acid, and sodium hydroxide as activation agents to activate rice husk carbon [18, 19, 20]. In this study, potassium hydroxide (KOH) was selected as the activation agent to increase the pore volume and adsorption capacity of the adsorbent water vapor [21]. The activation agent concentration and the activation time were studied to assess the water vapor adsorption property.

2. EXPERIMENTAL PROCEDURES

2.1. Materials

Rice husk char was bought from a local shop in Pedurungan, Semarang, Central Java. The char was sun-dried before being activated. The experiment was conducted using potassium hydroxide (90% purity, technical grade), hydrochloric acid (concentration of 32%, technical grade), distilled water, iodine solution (concentration of 1%, Merck & Co., Inc.), sodium thiosulfate (98% purity, Merck & Co., Inc.), and amylum (99% purity, Merck & Co., Inc.). Commercial adsorbents that were used as a comparison were coal-based commercial activated carbon (size of 4 – 8 mesh), white silica gel (size of 2 – 4 mm), and natural zeolite bought from a local shop (CV. Indrasari, Semarang, Central Java).

2.2. Carbon Activation

Before activation, rice husk char was prepared by pulverizing and sieving to 20 and 25 mesh. Char activation was conducted by adding 25 grams of rice husk char to 150 mL of 5% w/v KOH solution and letting it stand for 8 hours. The activated char (activated carbon) was filtered and washed using HCl and distilled water until the washing solution achieved a neutral pH. The wet activated carbon was dried in an oven at 110°C to the achievement of a constant mass and was placed in a desiccator. The activation procedure was repeated using KOH solution at different concentrations (10, 15, and 20% w/v) and activation times (2, 4, and 6 hours).

2.3. Iodine Number Adsorption

The iodine adsorption experiment was begun by mixing the activated carbon and 0.1 N iodine solution for 10 minutes. After the filtration, 10 mL of filtrate was titrated with 0.1 N sodium thiosulfate ($Na_2S_2O_3$) until became light yellow. The solution was then titrated by 1% amylum until clear from the blue color. The iodine adsorption capacity was calculated by the equation of (Suliestyah et al., 2020)

$$\text{Iodine number} = \frac{(V_1N_1 - V_2N_2)126.9\times 5}{W} \quad (1)$$

with V_1 and V_2 are volume of iodine and sodium thiosulfate (mL), respectively, N_1 is the normality of iodine (N), N_2 normality of sodium thiosulfate (N), and W is the mass of the sample (g).

2.4. Adsorption Capacity

Fig. 1 describes the experimental setup of the adsorption test. The adsorption capacity of the produced activated carbon was evaluated by placing 10 grams of activated carbon in an isolated mason jar. Previously, the jar was filled with a specific amount of water. The adsorption capacity was the total mass of water adsorbed into the sample that was measured by the gravimetric method. This test was conducted under temperatures of 15°C, room temperature (27°C), and 40°C for several days until equilibrium. In comparison, several commercial adsorbents were also examined with iodine and water vapor adsorption. The adsorption kinetics was evaluated using several models presented in Table 1. The adsorption capacity of prepared activated carbon

[DOI: 10.22068/ijmse.3522]

was then compared to other commercial adsorbents (commercial activated carbon, natural zeolite, and silica gel).

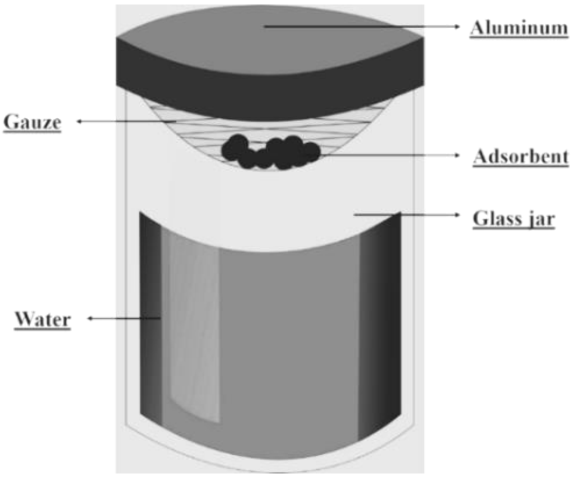

Fig. 1. Experimental set-up of the adsorption capacity evaluation

2.5. Materials Characterization

The functional groups in the activated carbon samples were examined using Fourier Transform Infrared (FTIR) employing PerkinElmer Frontier Infrared Spectrometer version 10.6.1, with a resolution of 1 cm^{-1} in a region of 400 to 4000 cm^{-1}. X-ray diffractions (XRD PANalytical X'Pert PRO, Malvern Panalytical Ltd.) with CuKα radiation of 1.54060Å were used to investigate the crystallinity of natural zeolite. This instrument operated at 40 kV, 30 mA, and the diffractograms were observed from 10.03° to 82.19° on a 2θ scale with a 0.7° step size. The chemical compositions of natural zeolite were observed using X-ray Fluorescence (Panalytical Minipal 4, Malvern Panalytical Ltd.). Three random samples were taken from the same source as the zeolite samples, named Zeolite A, B, and C. The crystal structure and the chemical composition of natural zeolite were shown in XRD patterns and XRF analysis in Fig. 2. According to XRD patterns evaluated by Highscore plus 3.0e (PANalytical B.V., The Netherlands), the peaks of zeolite samples indicate similar crystal structure (mordenite). This result was compatible with XRF analysis that showed a common compound of mordenite mineral $(Na_2, Ca, K_2) Al_2Si_{10}O_{24}\cdot 7H_2O$ [22].

3. RESULTS AND DISCUSSION

3.1. Fourier Transform Infrared (FTIR) Characterization

Fig. 4 shows the FTIR spectra of rice husk char and activated carbon, which highlight the chemical functional groups. Several functional groups with water affinity were discovered by this characterization, as well as some water that had bound to the activated carbon.

Table 1. Adsorption kinetics equation [22], [23]

Model	Equation
Pseudo-first-order	$q_t = q_e(1 - e^{-k_1 t})$
Pseudo-second-order	$q_t = \frac{k_2 {q_e}^2 t}{1 + k_2 q_e t}$
Notes: q_t= moisture adsorption at a certain time; q_e= moisture adsorption at equilibrium; t= adsorption time; k_1= constant parameter of pseudo-first-order; k_2= constant parameter of pseudo-second-order	

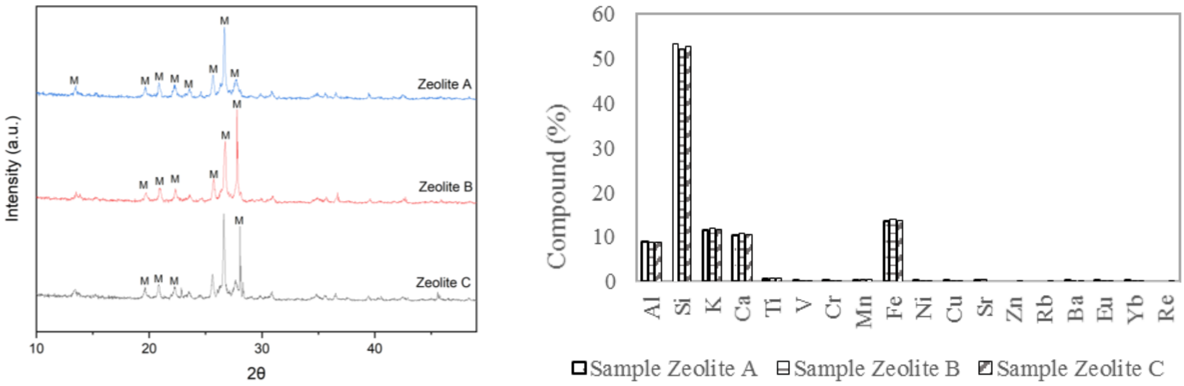

(a) (b)

Fig. 2. a) XRD patterns of natural zeolite used in this study b) compounds found in natural zeolite used in this study

[DOI: 10.22068/ijmse.3522]

A clear difference between the two samples was a higher peak of aromatic ring C=C at 1600–1500 cm^{-1} in the activated carbon and a C-O band of rice husk char at 1300–1050 cm^{-1} [23]. A C-H functional group at a wavenumber of 1374 cm^{-1} corresponds to bending vibrations in methyl groups [24]. It also found a higher broad peak in the range of wavenumber of 3600–3200 cm^{-1}, representing the O-H functional group and indicating the moisture-enriched surface of the activated carbon [13]. The oxygen-containing functional groups could fasten the water vapor adsorption performance of the activated carbon [24].

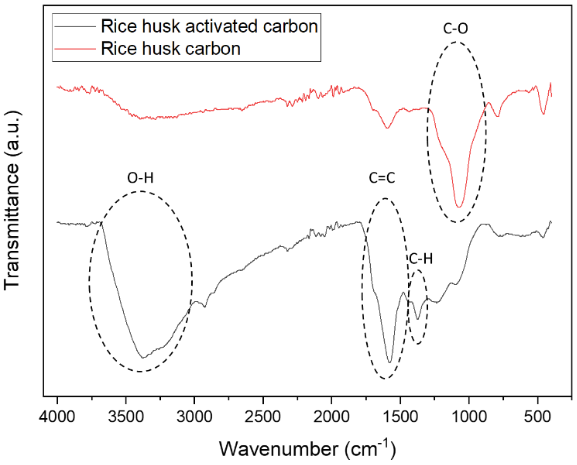

Fig. 3. FTIR spectra of rice husk char and activated carbon

3.2. Iodine Adsorption

According to Mianowski et al. [25], iodine adsorption represents the surface area of activated carbon for a range of 200–850 mg/g iodine number. Therefore, the surface area of rice husk activated carbon in this study was around 615 m^2/g and higher than other tested commercial adsorbents (Fig. 5).

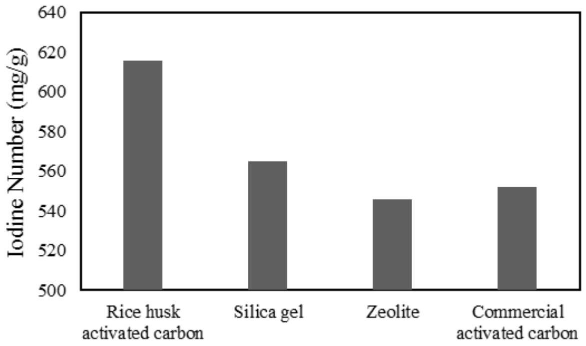

Fig. 4. Iodine adsorption of several adsorbents

According to this result, the product is highly potential to be as a high-capacity water vapor adsorbent. However, this result was still lower than nano-porous carbon with iodine adsorption of more than 700 mg/g [20]. This result indicates that the activated carbon product from this experiment had a higher lack of well-developed porosity than that of nano-porous carbon from rice husk.

3.3. Effect of Potassium Hydroxide Concentration

In the activation stage, the chemical reaction that occurred was [26]

$$6KOH + 2C \rightarrow 2K + 3H_2 + 2K_2CO_3 \tag{2}$$

Based on the reactions, KOH and carbon decomposed into potassium compounds (K and K_2CO_3) and hydrogen. The activated carbon was then washed with acid and water to remove them, clearing carbon pores [27]. Therefore, the water vapor adsorption of carbon was increased after the activation (Fig. 5). Untreated rice husks possessed the lowest adsorption capacity (0.04 g water/g adsorbent). Fig. 5 also presents water vapor adsorption of the activated carbon that was treated using different KOH concentrations for 8 hours. The data shows that manufacturing activated carbon using higher KOH concentration impacted a higher adsorption capacity. The highest adsorption capacity (0.42 g vapor/g adsorbent) belonged to activated carbon obtained from activation using 20% w/v KOH solution, and the lowest was found at 5% w/v KOH solution. This finding confirmed the FTIR characterization that showed a hydroxyl functional group on the activated carbon. Also, the theory states that a higher activation agent concentration facilitates higher carbon degradation to produce more pores [28]. However, the produced activated carbon was still lower than activated carbon derived from coffee shells [24] and tobacco stems [29]. The significance of different concentrations and adsorption times were evaluated with ANOVA summarized in Table 2, showing a significant impact of both factors (p-value< 0.05).

3.4. Effect of Activation Time

The analysis of the activation time was conducted for activated carbon that was activated using 20% w/v KOH solution for 2–8 hours. Fig. 6 depicts the adsorption capacity at different activation times.

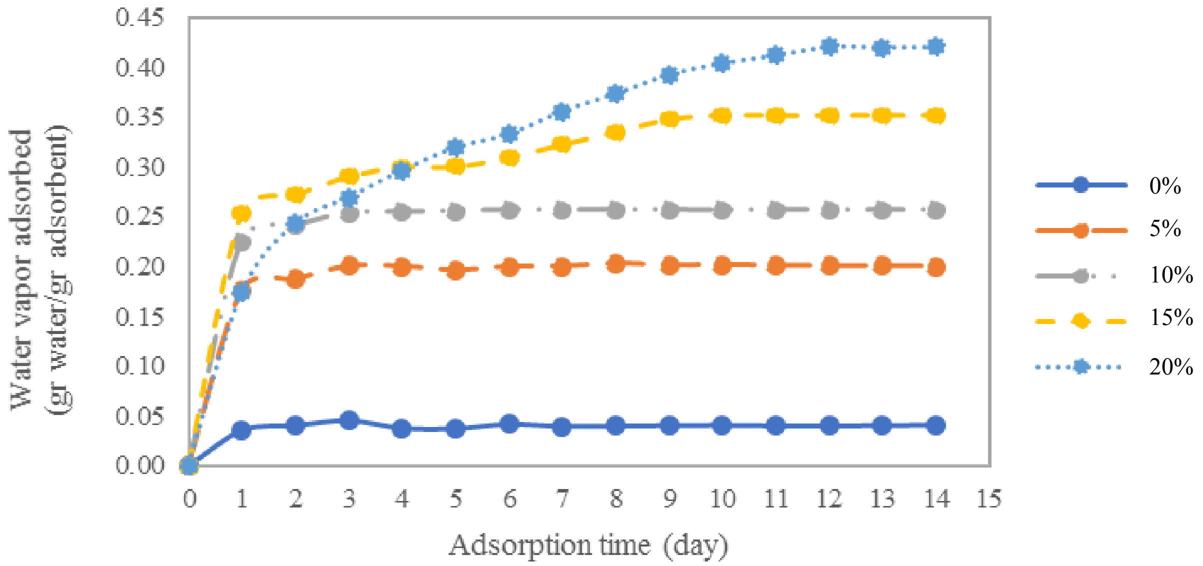

Fig. 5. Water vapor adsorption of activated carbon at different concentrations

Table 2. Two-way ANOVA of water vapor adsorption of the activated carbon at different adsorption times and KOH concentrations

Source of Variation	SS	df	MS	F	*P-value*	F crit
Adsorption time	28.9739	14	2.0696	10.7222	< 0.001	1.8726
Concentration	77.3276	4	19.3319	100.1570	< 0.001	2.5366
Error	10.8089	56	0.1930			
Total	117.1103	74				

The highest adsorption capacity was achieved at 8 hours of carbon activation (0.420 g vapor adsorbed/g adsorbent). Compared to the untreated rice husk char, activating the carbon for 8 hours increased the adsorption capacity up to 9 times. Analysis of the variance of this result also demonstrated that varying the activation period has a significant effect on the adsorption capacity (Table 3). Previous studies reported a different relationship between the activation time and adsorption capacity [24], [28]. Sun et al. [24] stated that changes in activation time did not have a significant effect on the maximum adsorption capacity. In contrast, Yang et al. [28] found a fluctuation in the adsorption capacity of activated carbon at different activation times. From a range of 0.5 to 3.0 hours, the maximum methylene blue adsorption was at 2 hours. That result occurred because of an excessive increase in reaction rate between KOH and carbon causing a higher growth of porous structure. Extending the activation duration can increase the contaminant's degradation and maximize the microporous formation [30].

3.5. Effect of Adsorption Temperature

The effect of adsorption temperature on the water vapor adsorption capacity of activated carbon was presented in Fig. 8. The test observed that a change of temperature of 15 °C to 27°C affected the adsorption capacity. At 40°C, there was no significant difference in the maximum water vapor adsorption capacity. More details, ANOVA indicated that the adsorption temperature and time had a significant effect on the water vapor adsorption (Table 4). Before, Chairunnisa et al. [12] and Cardenas et al. [31] explored the water vapor adsorption of activated carbon at 20-40°C.

Table 3. Two-way ANOVA of water vapor adsorption of the activated carbon at different activation times

Source of Variation	SS	df	MS	F	*P-value*	F crit
Adsorption time	30.0561	14	2.1469	13.3901	< 0.001	1.8726
Activation time	66.2628	4	16.5657	103.3209	< 0.001	2.5366
Error	8.9786	56	0.1603			
Total	105.2976	74				

[DOI: 10.22068/ijmse.3522]

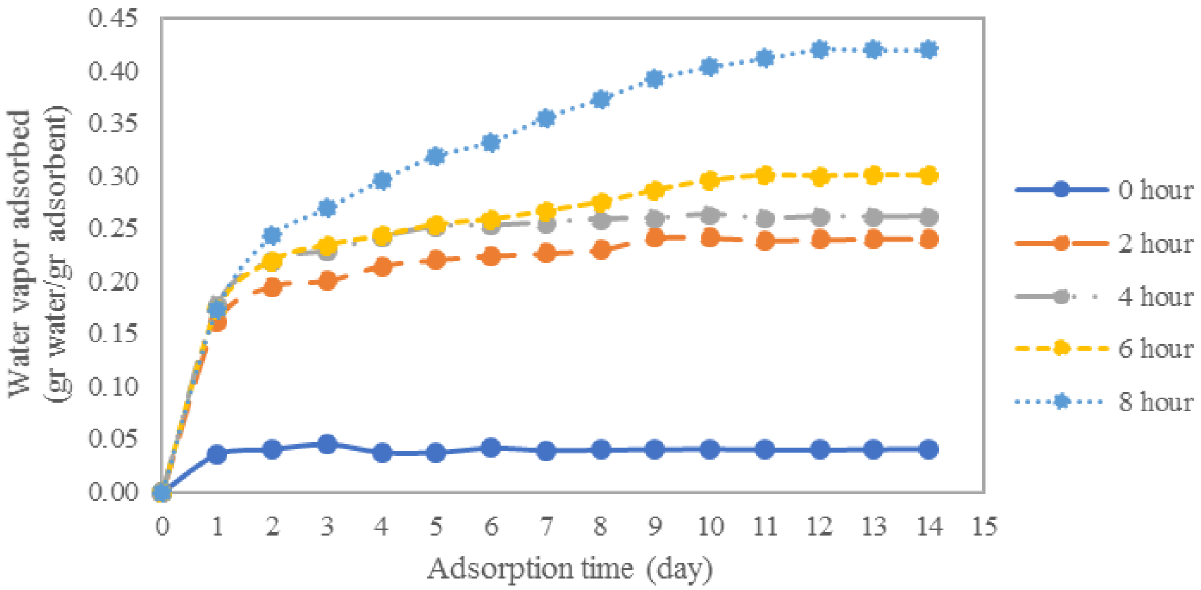

Fig. 6. Water vapor adsorption capacities at different activation times

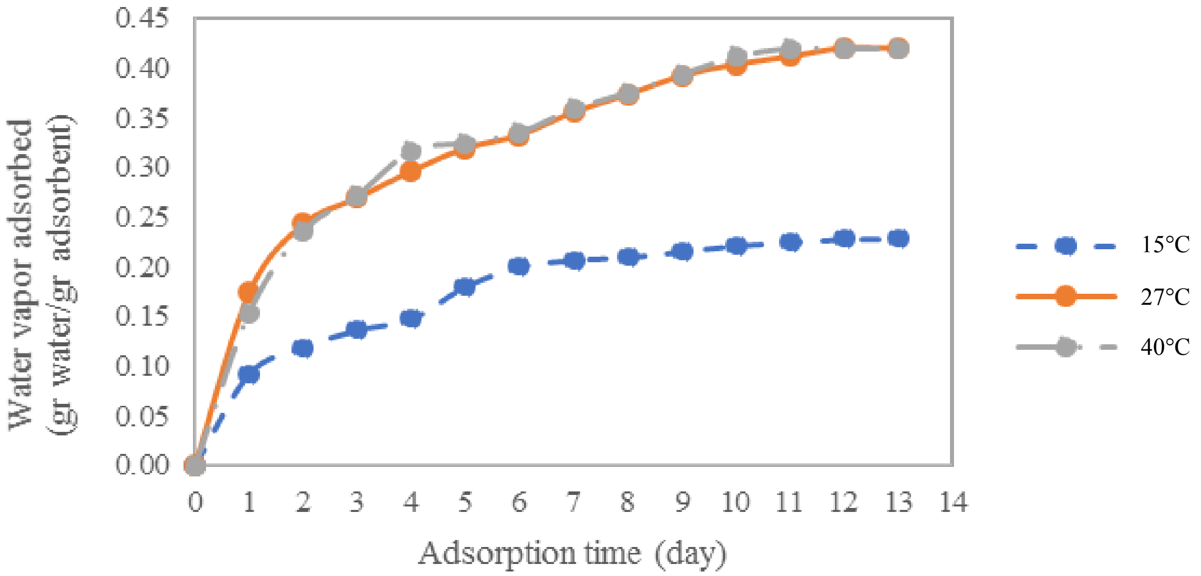

Fig. 7. Water vapor adsorption capacity at different temperatures

Table 4. Two-way ANOVA of water vapor adsorption capacity of the activated carbon at different temperatures

Source of Variation	SS	df	MS	F	*P-value*	F crit
Time	0.3975	13	0.0306	31.5170	< 0.001	2.1192
Temperature	0.1939	2	0.0970	99.9622	< 0.001	3.3690
Error	0.0252	26	0.0010			
Total	0.6166	41				

They found that increasing the adsorption temperature caused a reduction in the adsorption capacity. Combined with our results, the phenomenon that happened was a rapid formation of water clusters at temperatures lower than 30°C, and at higher temperatures, this water cluster became less stable [12]. Higher temperatures sped up the movement of water molecules and reduced the attraction of adsorbent and water [32].

Fig. 8 displays the effect of the adsorption temperature of several adsorbents. Interestingly, different adsorbents exhibited a different relationship. For example, when the temperature

[DOI: 10.22068/ijmse.3522]

increased from 15°C to 40°C, the maximum adsorption capacity of commercial activated carbon decreased by 33%. Moreover, the adsorption capacity of other adsorbents increased when the temperature increased from 15°C to 40°C. Also, this comparison indicated that the produced activated carbon from rice husk adsorbed more water vapor than other tested commercial adsorbents. This result was in agreement with the iodine adsorption test that showed a higher surface area of rice husk-activated carbon than other adsorbents.

3.6. Adsorption Kinetics

The adsorption kinetics of prepared activated carbon (20% w/v KOH solution and 8 hours activation) was evaluated by pseudo-first- and pseudo-second-order models. The kinetic study was analyzed by varying the adsorption temperature at 15°C, 27°C, and 40°C. The parameters of the two models are provided in Table 5. The most suitable model was determined by coefficient of determination (R^2) and SSE. Based on the calculation, two models show good fits with R^2 close to 1.0 and SSE close to 0. Furthermore, the pseudo-first-order model described the adsorption mechanism of activated carbon prepared at the highest concentration and longest activation time was better than the second-order (R^2 values closer to 1 and SSE closer to 0). It implied that the main mechanism for the adsorption of water vapor on that activated carbon was physisorption. Meanwhile, the pseudo-second-order model described some samples better than the first-order, agreeing with the chemisorption process [33].

4. CONCLUSIONS

Activated carbon from rice husks was activated by varying the concentration of KOH as the activation agent and the activation time.

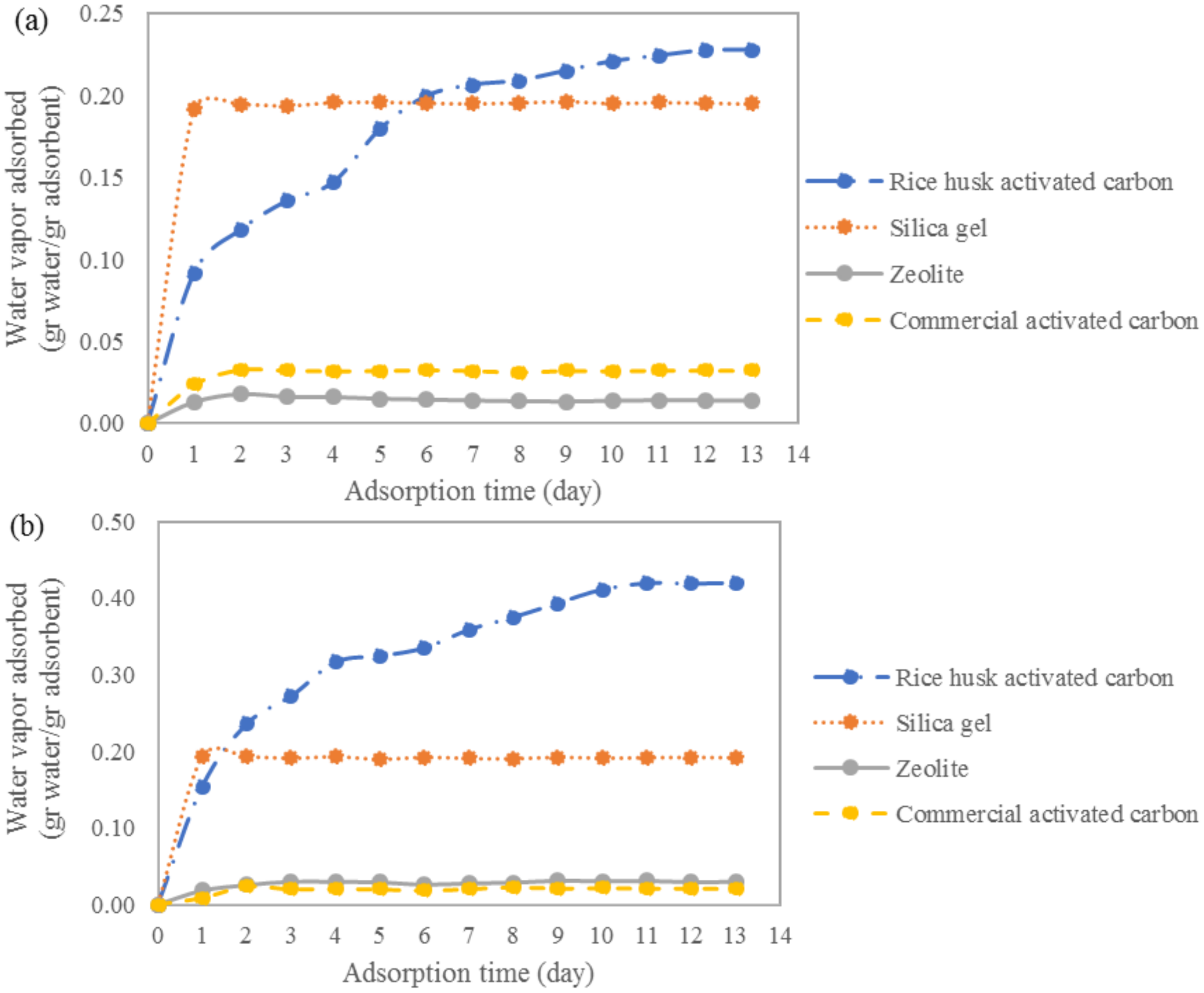

Fig. 8. Water vapor adsorption of several adsorbents at temperatures of (a) 15°C, (b) 40°C

[DOI: 10.22068/ijmse.3522]

Table 5. Parameters of non-linear pseudo-first- and pseudo-second-order model

Concentration (% w/v)	Pseudo-First-Order				Pseudo-Second-Order			
	k_1	q_e	R^2	SSE	k_2	q_e	R^2	SSE
5	0.0013	0.2001	0.8383	$9.6\text{x}10^{-6}$	0.0240	0.2001	0.8921	$1.9\text{x}10^{-5}$
10	0.0009	0.2572	0.9396	$6.3\text{x}10^{-5}$	0.0714	0.2569	0.9551	$4.5\text{x}10^{-5}$
15	0.0005	0.3506	0.6702	0.0008	0.0034	0.3506	0.8340	0.0002
20	0.0002	0.4184	0.9618	0.0006	0.0012	0.4184	0.9492	0.0007
Activation time (hour)								
2	0.0003	0.2405	0.9614	0.0006	0.0078	0.2405	0.9561	$6.0\text{x}10^{-5}$
4	0.0003	0.2656	0.9864	0.0008	0.0062	0.2656	0.9905	$3.0\text{x}10^{-5}$
6	0.0003	0.3013	0.8805	0.0005	0.0031	0.3013	0.9309	0.0001
8	0.0002	0.4184	0.9613	0.0006	0.0010	0.4184	0.9532	0.0008
Temperature (°C)								
15	0.0002	0.2326	0.9686	0.0001	0.0019	0.2326	0.9398	0.0003
27	0.0002	0.4184	0.9613	0.0006	0.0010	0.4184	0.9532	0.0008
40	0.0003	0.4224	0.9425	0.0007	0.0009	0.4224	0.9772	0.0011

The Fourier transform infrared (FTIR) spectral characterization represents that there was a significant effect on the activation of rice husk activated carbon as indicated by differences in functional groups before and after activation, including the addition of the hydroxyl group which made the activated carbon more hydrophilic, and the presence of the C=C group indicated an increase in carbon content. Based on the iodine adsorption test, the surface area of the activated carbon produced was around 615 m^2/g. The adsorption test showed that an increase in KOH concentration of up to 20% (w/v) and an activation time of 8 hours increased the adsorption capacity of the resulting activated carbon up to 0.420 g/g. Adsorption was also examined at 15°C, 27°C, and 40°C and showed an increase in adsorption capacity with increasing temperature. The produced activated carbon that was activated using 20% w/v KOH for 8 hours showed a good fit with the pseudo-first-order adsorption kinetics model. According to the comparison, activated carbon from rice husk showed a higher adsorption capacity than silica gel, zeolite, and commercial activated carbon. This research found that activated carbon from rice husks is a promising material to be applied to the dehumidification system.

ACKNOWLEDGEMENT

This research was funded by Diponegoro University contract number 118-24/UN7.6.1/PP-22.

REFERENCES

[1]. Sleiti, A. K., Al-Khawaja, H., Al-Khawaja, H. and Al-Ali, M., "Harvesting Water from Air Using Adsorption Material–Prototype and Experimental Results." Sep. Purif. Technol., 2021, 257, 117921.

[2]. Wang, C., Yang, B., Ji, X., Zhang, R. and Wu, H., "Study on Activated Carbon/ Silica Gel/Lithium Chloride Composite Desiccant for Solid Dehumidification." Energy, 2022, 251, 123874.

[3]. Djaeni, M. and Perdanianti, A. M., "The Study Explores the Effect of Onion (Allium Cepa L.) Drying Using Hot Air Dehumidified by Activated Carbon, Silica Gel and Zeolite." J. Phys.: Conf. Ser., 2019, 1295, 012025.

[4]. Xia, X., Liu, Z. and Li, S., "Adsorption Characteristics and Cooling/Heating Performance of COF-5." Appl. Therm. Eng., 2020, 176, 115442.

[5]. Ashraf, S., Sultan, M., Bahrami, M., McCague, C., Shahzad, M. W., Amani, M., Shamshiri, R. R. and Ali, H. M., "Recent Progress on Water Vapor Adsorption Equilibrium by Metal-Organic Frameworks for Heat Transformation Applications." Int. Commun. Heat and Mass Transf., 2021, 124, 105242.

[6]. Moura, P. A. S., Rodríguez-Aguado, E., Maia, D. A. S., Melo, D. C., Singh, R., Valencia, S., Webley, P. A., Rey, F., Bastos-Neto, M., Rodríguez-Castellón, E. and Azevedo, D. C. S., "Water Adsorption and Hydrothermal Stability of CHA Zeolites with Different Si/Al Ratios and

Compensating Cations." Catal. Today, 2022, 390–391, 99–108.
[7]. Zheng, X., Chen, K. and Lin, Z., "Synthesis and Characterization of Alginate–Silica Gel Composites for Adsorption Dehumidification." Ind. Eng. Chem. Res., 2020, 59, 5760–5767.
[8]. A'yuni, D. Q., Subagio, A., Hadiyanto, H., Kumoro, A. C. and Djaeni, M., "Microstructure Silica Leached by NaOH from Semi-Burned Rice Husk Ash for Moisture Adsorbent." Arch. Mater. Sci. Eng., 2021, 1, 5–15.
[9]. Sun, S., Yu, Q., Li, M., Zhao, H., Wang, Y. and Ji, X., "Effect of Carbonization Temperature on Characterization and Water Vapor Adsorption of Coffee-Shell Activated Carbon." Ads. Sci. Technol., 2020, 38, 377–392.
[10]. Zu, K. and Qin, M., "Experimental and Modelling Investigation of Water Adsorption of Hydrophilic Carboxylate-Based MOF for Indoor Moisture Control." Energy, 2021, 228, 120654.
[11]. Gargiulo, N., Peluso, A. and Caputo, D., "MOF-Based Adsorbents for Atmospheric Emission Control: A Review." Processes, 2020, 8, 613.
[12]. Chairunnisa, Miksik, F., Miyazaki, T., Thu, K., Miyawaki, J., Nakabayashi, K., Wijayanta, A. T. and Rahmawati, F., "Development of Biomass Based-Activated Carbon for Adsorption Dehumidification." Energy Rep., 2021, 7, 5871–5884.
[13]. Liu, Z., Sun, Y., Xu, X., Qu, J. and Qu, B., "Adsorption of Hg(II) in An Aqueous Solution by Activated Carbon Prepared from Rice Husk Using KOH Activation." ACS Omega, 2020, 5, 45, 29231–29242.
[14]. Wazir, A. H., Ullah, I. and Yaqoob, K., "Chemically Activated Carbon Synthesized from Rice Husk for Adsorption of Methylene Blue in Polluted Water." Environ. Eng. Sci., 2023, 40, 307–317.
[15]. Sintawardani, N., Adhilaksma, C. A., Hamidah, U., Pradanawati, S. A. and Suharno, S. M., "Evaluation of Human Urine Purification Using Rice Husk Charcoal as The Adsorbent." IOP Conf. Ser.: Earth Environ. Sci., 2023, 1201, 012107.
[16]. Warsiki, E., Agriawati, D., Noor, E. and Iskandar, A., "Isotherm Moisture Sorption of Composite Desiccant Made from Rice Husk Biomass." IOP Conf. Ser.: Earth Environ. Sci., 2021, 749, 012011.
[17]. Chirsty, A. A. and Sivarukshy, P., "Comparison of Adsorption Properties of Commercial Silica and Rice Husk Ash (RHA) Silica: A Study by NIR Spectroscopy," Open Chem., 2021, 19, 426–431.
[18]. Emdadi, Z., Asim, N., Yarmo, M. A, Ebadi, M., Mohammad, M. and Sopian, K., "Chemically Treated Rice Husk Blends as Green Desiccant Materials for Industrial Application." Chem. Eng. Technol., 2017, 40, 1619–1629.
[19]. He, S., Chen, G., Xiao, H., Shi, G., Ruan, C., Ma, Y., Dai, H., Yuan, B., Chen, X. and Yang., X., "Facile Preparation of N-Doped Activated Carbon Produced from Rice Husk for CO_2 Capture." J. Colloid Interface Sci., 2021, 582, 90–101.
[20]. Shrestha, L., Thapa, M., Shrestha, R., Maji, S., Pradhananga, R. and Ariga, K., "Rice Husk-Derived High Surface Area Nanoporous Carbon Materials with Excellent Iodine and Methylene Blue Adsorption Properties." C Journal of Cabon Research, 2019, 5, 10.
[21]. Liu, Y., Huo, Z., Song, Z., Zhang, C., Ren, D., Zhong, H. and Jin, F., "Preparing a Magnetic Activated Carbon with an Expired Beverage as Carbon Source and KOH as The Activator." J. Taiwan Inst. Chem. Eng., 2019, 96, 575–587.
[22]. Gurses, A., Dogar, C., Yalcin, M., Acikyildiz, M., Bayrak, R. and Karaca, S., "The Adsorption Kinetics of The Cationic Dye, Methylene Blue, Onto Clay." J. Hazardous Materials, 2006, 131 (1–3), 217–228.
[23]. Qiu, H., Lv., L., Pan, B., Zhang, Q., Zhang, W. and Zhang, Q., "Critical Review in Adsorption Kinetic Models," J. Zhejiang Univ. Sci. A, 2009, 10 (5), 716–724.
[24]. Philia, J., Widayat, W., Sulardjaka, S., Nugroho, G. A. and Darydzaki, A. N., "Aluminum-Based Activation of Natural Zeolite for Glycerol Steam Reforming." Results Eng., 2023, 19, 101247.

[DOI: 10.22068/ijmse.3522]

[25]. Muslim, A., Purnawan, E., Meilina, H., Azwar, M. Y., Deri, N. O. and Kadri, A., "Adsorption of Copper Ions onto Rice Husk Activated Carbon Prepared Using Ultrasound Assistance: Optimization Based on Step-by-Step Single Variable Knockout Technique." J. Eng. Sci. Technol., 2022, 17, 2496–2511.

[26]. Sun, S., Yu, Q., Li, M., Zhao, H. and Wu, C., "Preparation of Coffee-Shell Activated Carbon and Its Application for Water Vapor Adsorption." Renew. Energy, 2019, 142, 11–19.

[27]. Mianowski, A., Owczarek, M. and Marecka, A., "Surface Area of Activated Carbon Determined by the Iodine Adsorption Number." Energy Sources, Part A: Recovery, Utilization, and Environmental Effects, 2007, 29, 839–850.

[28]. Linares-Solano, A., Lillo-Ródenas, M. A., Marco-Lozar, J. P., Kunowsky, M. and Romero-Anaya, A. J., "NaOH and KOH for Preparing Activated Carbons Used in Energy and Environmental Applications." Int. J. Energy, Environment and Economics, 2012, 20, 59–91.

[29]. Oginni, O., Singh, K., Oporto, G., Dawson-Andoh, B., McDonald, L. and Sabolsky, E., "Influence of One-Step and Two-Step KOH Activation on Activated Carbon Characteristics." Bioresour. Technol. Rep., 2019, 7, 100266.

[30]. Yang, H. M., Zhang, D. H., Chen, Y., Ran, M. J. and Gu, J. C., "Study on The Application of KOH to Produce Activated Carbon to Realize the Utilization of Distiller's Grains." IOP Conf. Ser: Earth Environ. Sci., 2017, 69.

[31]. Yu, Q., Zhao, H., Zhao, H., Sun, S., Ji, X., Li, M. and Wang, Y., "Preparation of Tobacco-Stem Activated Carbon from Using Response Surface Methodology and Its Application for Water Vapor Adsorption in The Solar Drying System." Sol. Energy, 2019, 177, 324–336.

[32]. Liang, Q., Liu, Y., Chen, M., Ma, L., Yang, B., Li, L. and Liu, Q., "Optimized Preparation of Activated Carbon from Coconut Shell and Municipal Sludge." Mater. Chem. Phys., 2020, 241, 122327.

[33]. Cardenas, C., Farrusseng, D., Daniel, C. and Aubry, R., "Modeling of Equilibrium Water Vapor Adsorption Isotherms on Activated Carbon, Alumina and Hoplite." Fluid Phase Equilib., 2022, 561, 113520.

[34]. Wang, T., Tian, S., Li, G., Sheng, M., Ren, W., Liu, Q., Tan, Y. and Zhang, P., "Experimental Study of Water Vapor Adsorption Behaviors on Shale." Fuel, 2019, 248, 168–177.

[35]. Robati, D., "Pseudo-Second-Order Kinetic Equations for Modelling Adsorption Systems for Removal of Lead Ions Using Multi-Walled Carbon Nanotube," J. Nanostruct. Chem., 2013, 3, 55.

[DOI: 10.22068/ijmse.3522]